Early life stress-induced alterations in the activity and morphology of ventral tegmental area neurons in female rats

Jadwiga Spyrka [a,1], Anna Gugula [a,1], Agnieszka Rak [b], Grzegorz Tylko [c], Grzegorz Hess [a,**], Anna Blasiak [a,*]

[a] Department of Neurophysiology and Chronobiology, Institute of Zoology and Biomedical Research, Jagiellonian University, 30-387, Krakow, Poland
[b] Department of Physiology and Toxicology of Reproduction, Institute of Zoology and Biomedical Research, Jagiellonian University, 30-387, Krakow, Poland
[c] Department of Cell Biology and Imaging, Institute of Zoology and Biomedical Research, Jagiellonian University, 30-387, Krakow, Poland

A R T I C L E   I N F O

A B S T R A C T

Childhood maltreatment, which can take the form of physical or psychological abuse, is experienced by more than a quarter of all children. Early life stress has substantial and long-term consequences, including an increased risk of drug abuse and psychiatric disorders in adolescence and adulthood, and this risk is higher in women than in men. The neuronal mechanisms underlying the influence of early life adversities on brain functioning remain poorly understood; therefore, in the current study, we used maternal separation (MS), a rodent model of early-life neglect, to verify its influence on the properties of neurons in the ventral tegmental area (VTA), a brain area critically involved in reward and motivation processing. Using whole-cell patch-clamp recordings in brain slices from adolescent female Sprague-Dawley rats, we found an MS-induced increase in the excitability of putative dopaminergic (DAergic) neurons selectively in the medial part of the VTA. We also showed an enhancement of excitatory synaptic transmission in VTA putative DAergic neurons. MS-induced alterations in electrophysiology were accompanied by an increase in the diameter of dendritic spine heads on lateral VTA DAergic neurons, although the overall dendritic spine density remained unchanged. Finally, we reported MS-related increases in basal plasma ACTH and corticosterone levels. These results show the long-term consequences of early life stress and indicate the possible neuronal mechanisms of behavioral disturbances in individuals who experience early life neglect.

1. Introduction

Childhood stressful experiences have been shown to interfere with normal brain development (Andersen, 2019; Gershon et al., 2013; Green et al., 2010). The consequences of exposure to adversity in early life are associated with complex changes in reward processing in adolescence and adulthood, including hyporesponsiveness during reward anticipation and hyperresponsiveness when receiving a reward (Boecker et al., 2014; reviewed in Novick et al., 2018). Adverse effects of early life trauma can be observed particularly in adolescence, manifested by higher risk of violent behavior, substance abuse, suicide attempt and increased vulnerability to neurological disorders (Andersen, 2019; Fergusson et al., 2000; Kessler et al., 1997; World Health Organization, 2020). Moreover, early life adversity-related risk of substance abuse,

relapse to drug abuse, depression and anxiety has been reported to be higher in women than in men (reviewed in Forster et al., 2018).

Dopaminergic (DAergic) neurons in the ventral tegmental area (VTA) play a major role in reward and motivation processing as well as in the formation of long-term memory traces (reviewed in Lisman and Grace, 2005; Pignatelli and Bonci, 2015; Salamone et al., 2016). Thus, early life stress-induced disturbances in these processes appear to be related, at least partially, to altered functional connectivity between the VTA and hippocampus (Pruessner et al., 2004; Marusak et al., 2017) as well as to increased stress-related DAergic activity in the cerebral cortex and the ventral striatum of those who experience early childhood trauma (Kasanova et al., 2016). Another well-known effect of early life adversity is disturbed development of the hypothalamic-pituitary-adrenal (HPA) axis that results in altered

---

responsiveness to different types of stressors in individuals who experience childhood maltreatment (Heim et al., 2008). The underlying neurochemical and cellular mechanisms remain to be fully elucidated.

An experimental tool for studying the effects of early life stress is maternal separation (MS) of rodent pups. MS has been demonstrated to affect brain growth and development and to evoke anxiety-like and depressive behaviours as well as to decrease social interactions (reviewed in Bonapersona et al., 2019; Lippmann et al., 2007; Nishi et al., 2014). MS-induced long-lasting behavioral alterations also include impairment of the ability to learn reward value (Stuart et al., 2019). A potential mechanism underlying these changes is a modification in the activity of VTA DAergic neurons that rapidly respond to both rewarding and aversive stimuli (Holly and Miczek, 2016). MS also induces changes in the responsiveness of DA neurons to aversive stimuli later in life. The nature of these changes may depend on the type of stressor, as both increases (Brake et al., 2004) and decreases (Jahng et al., 2010) in DAergic system reactivity to different acute stressors have been reported in maternally stressed rats. In mice, MS during a specific postnatal period increases susceptibility to adult social defeat stress and induces long-lasting transcriptional modifications in the VTA, leading to a "depression-like state" (Peña et al., 2017). Little is known about the long-term consequences of MS on the structure and function of VTA DAergic neurons. MS during the first two postnatal weeks has been reported to increase the number of tyrosine hydroxylase (TH, the rate-limiting enzyme of catecholamine synthesis)-immunoreactive cells in the VTA of young adult female, but not male rats (Chocyk et al., 2011). MS also induces an increase in the density of TH-immunoreactive fibres in the prefrontal cortex and nucleus accumbens of adolescent female rats, and this effect is accompanied by changes in the levels of DA receptor mRNAs in target structures (Majcher-Maślanka et al., 2017).

VTA neuronal activity remains under the control of glutamatergic afferents, and the activation of ionotropic glutamate receptors induces burst firing of DAergic neurons in vivo (Chergui et al., 1993), which is critical for the effects of drugs of abuse and for reward-dependent learning (Zweifel et al., 2009). The VTA receives glutamatergic innervation originating from different brain areas ranging from the prefrontal cortex to the caudal brainstem (reviewed in Geisler et al., 2007). The sources of glutamatergic projections to the medial and lateral parts of the VTA differ, at least partially (reviewed in Juarez and Han, 2016) and both parts of the VTA send projections to different targets (Lammel et al., 2011, 2012). The exposure of adolescent and adult rodents to repeated stressors profoundly modifies excitatory synaptic transmission within the VTA, which has long-term consequences for the activity of VTA neurons and DA release in target structures (reviewed in Holly and Miczek, 2016; Polter and Kauer, 2014). However, it is unknown whether and how MS affects excitatory synaptic transmission and neuronal excitability of DAergic neurons in the VTA of adolescent rats. Since the majority of animal studies on the effects of MS are performed on males, female rats were used in the current study. We aimed to determine whether MS induces functional changes in excitatory synaptic inputs to putative DAergic and non-DAergic neurons in the medial and lateral parts of the VTA. Moreover, we compared the excitability of these cells, dendritic spines and the overall dendritic morphology of putative DAergic neurons in the medial and lateral parts of the VTA of MS-exposed and control animals. To verify the influence of MS on the HPA axis we assessed basal blood levels of adrenocorticotropic hormone (ACTH) and corticosterone (CORT).

2. Methods

2.1. Animals and treatment

The experiments were carried out using female Sprague-Dawley rats (housing facility of the Institute of Zoology and Biomedical Research, Jagiellonian University in Krakow, Poland). The experiments were approved by the 2nd Local Institutional Animal Care and Use Committee (Krakow, Poland) and carried out in accordance with the EU Directive 2010/63/EU on the protection of animals used for scientific purposes. All efforts were made to minimize the number of animals used and their suffering.

The day of birth was defined as postnatal day 0 (PND 0), and litters were standardized to a fixed number of 5–9 female pups. Dams were housed together with their offspring on a standard light/dark cycle (lights on: 8.00–20.00), temperature 22 °C, with food and water available ad libitum. In the MS group, every day from PND 2 to PND 14, the dams were removed from the maternity cages and housed individually in holding cages for 3 h (10:00–13:00). During this time, the litters were left in the home cages without additional heating, and afterwards, the dams were returned to the home cages (Danielewicz and Hess, 2014). In the control group, the pups were kept undisturbed with their mothers. Except for the separation procedure, animals from both groups were treated equally, including the same amount of handling during standard cage cleaning. Young animals were weaned on PND 28 and housed in family groups with 5–9 rats per cage. All subsequent experiments were performed on PND 42–56.

2.2. Brain slice preparation and whole-cell recording

Rats were deeply anaesthetised with isoflurane (Aerrane, Baxter, Poland) between 8:00 and 9:00 and then decapitated. A total of 41 control (from 12 litters) and 39 MS (from 8 litters) female offspring were included in the study. The remaining animals were used for other research projects. The brains were removed and placed in ice-cold modified artificial cerebrospinal fluid (ACSF) containing (in mM): 92 NaCl, 30.0 NaHCO$_3$, 1.25 NaH$_2$PO$_4$, 10.0 MgSO$_4$, 2.5 KCl, 0.5 CaCl$_2$, 20.0 HEPES, 5.0 Na + ascorbate, 3.0 Na$^+$ pyruvate, 2.0 thiourea and 10 glucose saturated with a mixture of 95% O$_2$ and 5% CO$_2$ (pH 7.3–7.4, osmolarity 290–310 mOsmol/L). Slices (200 μm thick) containing the VTA were cut in the horizontal plane using a vibrating microtome (VT 1000S Leica Microsystems, Germany). Next, the slices were transferred to a preincubation chamber with standard ACSF containing (in mM): 124 NaCl, 26 NaHCO$_3$, 1.25 NaH$_2$PO$_4$, 1 MgSO$_4$, 4.5 KCl, 1.8 CaCl$_2$ and 10 glucose. The slices were stored at 32 ± 0.2 °C for approximately 2 h prior to recordings.

After the recovery period, individual slices were placed in a submerged-type recording chamber, in which the tissue was continuously perfused (2 ml/min) with standard ACSF. The recording chamber was placed on a fixed stage of a Zeiss Axio Examiner A1 microscope (Zeiss, Germany) equipped with video-enhanced infrared-differential interference contrast (DIC) optics. Individual neurons were visualized using a $40\times/1.0$ water immersion lens. Whole-cell configuration was obtained using negative pressure delivered through recording micropipettes (8–11 MΩ) pulled from borosilicate glass capillaries (Sutter Instrument, USA) using a Sutter Instrument P97 puller. The pipette solution contained (in mM): 125 K-gluconate, 20 KCl, 2 MgSO$_4$, 10 HEPES, 4 Na$_2$-ATP, 0.4 Na-GTP, 5 EGTA and 0.05% biocytin (pH 7.2–7.3, osmolarity 290–300 mOsmol/kg). All reagents used for the ACSF and intrapipette solution were purchased from Sigma-Aldrich (Germany). The data were corrected for a calculated +12.4 mV liquid junction potential. Signals were recorded using an SEC-05X amplifier (NPI, Germany), filtered at 3 kHz, and digitized at 20 kHz using a Micro1401 converter (Cambridge Electronic Design (CED), UK) with Signal and Spike2 software (CED, RRID:SCR_017081 and RRID:SCR_000903, respectively).

2.2.1. Electrophysiological recordings and analysis

After obtaining whole-cell configuration, VTA neurons were current-clamped at −75 mV, and 500 m s rectangular current pulses of increasing amplitude from −140 pA to +140 pA (increments of 10 pA) were delivered every 5 s. Membrane resistance, the time constant (tau) and capacitance (Ce) as well as voltage sag (the difference in the voltage between the nadir and the plateau levels) were measured based on the

voltage response to the −140 pA hyperpolarizing pulse. The firing characteristics of the recorded cells were assessed using depolarizing current pulses from +10 pA to +140 pA. Action potential (AP) parameters, including the threshold, amplitude, rise time (10%–90% of maximum), half width, after-hyperpolarization (AHP) minimum and AP peak to AHP minimum time, were determined using the first action potential evoked by the smallest depolarizing current step. To measure the rheobase current, a 1 s depolarizing ramp current injection from 0.1 to 1 nA was used.

Spontaneous excitatory postsynaptic currents (sEPSCs) were recorded for at least 5 min as outward currents in the voltageclamp mode, at a holding potential of −70 mV. Input resistance was continuously monitored, and only cells with stable access resistance were used for data analysis. For further analysis, 120 s long segments were selected, and sEPSCs were detected off-line and analysed using Mini Analysis software (Synaptosoft, USA, RRID:SCR_002184). The peak currents of individual events were identified using an automatic detection protocol. The average baseline current was calculated for an interval between 3 and 5 m s before the peak, and the threshold amplitude of sEPSC detection was set to 8 pA. Next, recordings were inspected manually for correctness. Recorded events were characterized in terms of the mean frequency, amplitude, 10–90% rise time and decay time constant (tau).

2.2.2. Post-recording immunostaining

After recordings, brain slices were fixed overnight by immersion in 4% formaldehyde in phosphate buffered saline (PBS) at 4 °C. Next, the slices were washed 3 × 10 min in PBS and incubated in PBS solution containing 10% normal donkey serum (NDS) and 0.6% Triton X-100 (for blocking unspecific binding sites and permeabilization, respectively) for 3 h at room temperature. Afterwards, the slices were washed 1 × 10 min in PBS and incubated in PBS solution containing primary antibodies against TH (mouse anti-TH (F-11), 1:250, Santa Cruz Biotechnology, Cat# sc-25269, Lot# G1318, RRID:AB_628422), ExtrAvidin-Cy3 (biocytin binding protein, 1:200, Sigma-Aldrich, Cat# E4142, Lot# SLBT2189), 2% NDS and 0.3% Triton X-100 for 48–72 h at 4 °C. The slices were then washed 4 × 10 min in PBS and incubated in PBS solution containing 2% NDS and Alexa Fluor 647-conjugated donkey anti-mouse (1:400, Jackson ImmunoResearch Labs, Cat# 715-606-151, Lot# 138538, RRID:AB_2340866) or Alexa Fluor 488-conjugated donkey anti-mouse (1:400, Jackson ImmunoResearch Labs, Cat# 715-545-151, Lot# 127820, RRID:AB_2341099) secondary antibody for 24 h at 4 °C. After subsequent washing in PBS (4 × 10 min), the slices were mounted onto glass slides and coverslipped with aqueous mounting medium (Fluoroshield with DAPI, Sigma-Aldrich, Cat# F6057, Lot# SLCC1782, SLBX6915 or SLCC1782).

2.3. Assessment of dendritic morphology

TH-immunoreactive (TH-ir) cells filled with biocytin during recordings with complete, well-stained and clearly visible dendritic trees (control: 43 cells from 33 rats, MS: 37 cells from 25 rats) from both the medial and lateral VTA (medial VTA: 10 control and 10 MS neurons, lateral VTA: 33 control and 27 MS neurons) were imaged using a confocal laser microscope (LSM710 on AxioObserver Z1, Zeiss, Germany) with an EC Plan-Neofluar 20×/0.50 M27 objective with 0.6 or 0.8× digital zoom depending on the cell size (x and y scaling: 0.278 μm, optical section thickness: 2.348 μm). Subsequent dendritic tracing combined with 3D Sholl analysis (10 μm step size) was performed on the acquired images in ImageJ (Fiji, RRID:SCR_002285) (Schneider et al., 2012) with the Simple Neurite Tracer plugin (RRID:SCR_016566) (Longair et al., 2011). Other parameters describing dendritic trees (the number of primary dendrites, bifurcations, branches and dendritic tips, the total dendritic length and the maximal branch order) were obtained with L-Measure software (RRID:SCR_003487) (Scorcioni et al., 2008). Cells not immunoreactive for TH were not included in the analysis.

2.4. Dendritic spine counting and analysis

For dendritic spine counting, only well-stained neurons with visible dendritic spines were selected (medial VTA: 7 control and 9 MS neurons, lateral VTA: 32 control and 25 MS neurons, from a total of 31 control and 22 MS rats). Randomly chosen first, second and third order dendritic segments from each cell were imaged using a confocal microscope (LSM710 on AxioObserver Z1) with an EC Plan-Neofluar 100×/1.3 Oil M27 objective with 1.5× digital zoom. The z-stack images (528 × 528 pixel resolution, x and y scaling: 0.107 μm, optical section thickness: 0.496 μm) were then deconvolved with Huygens Professional software (version 4.2, SVI, Netherlands, RRID:SCR_014237). Deconvolutions were based on the experimental point spread function (PSF) developed from the set of distilled images of 0.175-μm fluorescent beads (PS-Speck Microscope Point Source Kit (P7220), Life Technologies, USA). Dendritic spines were counted by a blinded, unbiased experimenter using manual mode in NeuronStudio software (RRID:SCR_013798) (Rodriguez et al., 2008). Spine density was calculated on 7774.85 μm of control dendrites (mean dendritic length of each cell: 199.355 μm) and 5998.73 μm of MS dendrites (mean dendritic length of each cell: 176.433 μm) and analysed along with the measurements of the diameter of each spine head (medial VTA: 273 control and 374 MS spines, lateral VTA: 1843 control and 1015 MS spines).

2.5. Plasma hormone assay

Between 8:30 and 9:00 trunk blood from separate groups of control (n = 6 rats from 2 litters) and MS rats (n = 6 rats from 2 litters) was collected on ice in 2-ml plastic tubes containing 100 μl of 5% ethylenediaminetetraacetic acid (EDTA) in water. Blood plasma samples were prepared by low-speed centrifugation (2,000×g at 4 °C for 10 min) and stored at −80 °C until analysis. A commercially available rat corticosterone ELISA kit (Shanghai Sunred Biological Technology Co., Ltd., China, Cat# SRB-T-87473) and rat ACTH ELISA kit (Shanghai Sunred Biological Technology Co., Ltd., Cat# SRB-T-85106) were used to quantify corticosterone and ACTH levels in plasma, respectively. The sensitivity of the corticosterone assay was 5.005 ng/ml, and the inter- and intra-experimental coefficients of variation were <12% and <10%, respectively. The sensitivity of the ACTH assay was 5.226 ng/l, and the inter- and intra-experimental coefficients of variation were <12% and <10%, respectively. Samples were run in duplicate within the same assay.

2.6. Statistical analysis

Statistical analysis was performed using GraphPad Prism 6 (GraphPad Software, RRID:SCR_002798) or Sigma Plot 11.0 software (Systat Software Inc., RRID:SCR_003210). The action potential peak to AHP minimum times were analysed by the nonparametric Kruskal-Wallis test followed by Dunn's multiple comparison test. For further analysis, neurons were divided into eight groups based on the experimental group (control or MS), putative DAergic phenotype (putative DAergic neuron or non-DAergic neuron) and location within the slice (medial (M) or lateral (L), Fig. 1). The medial and lateral VTA were defined as the regions located medially or laterally in relation to the line halfway between the medial terminal nucleus of the accessory optical tract (MT) and the *fasciculus retroflexus* (fr, Fig. 1A) (Lammel et al., 2014). Data points detected by the ROUT method (Q = 5%) as outliers were excluded from the analysis. All data were pretested for normal distribution. Membrane properties, action potential shape, sEPSC kinetics and properties, and most morphological data were analysed using two-way ANOVA with cell location (medial or lateral) as the first factor and treatment (control or MS) as the second factor. The firing characteristics of the recorded cells were analysed by fitting either a sigmoidal curve [[y = a/(1 + exp(-(x-x0)/b))]] or linear regression [y = yIntercept + Slope*x] to the data when applicable. Next, F statistics were used to test
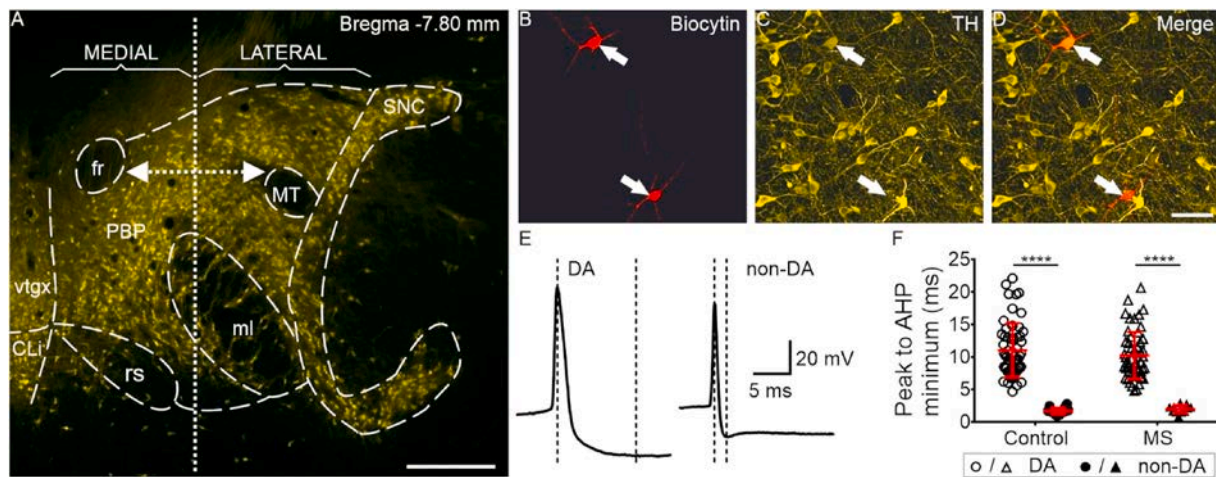
Fig. 1. Putative DAergic and putative non-DAergic VTA neurons have highly distinctive action potentials. **(A)** Microscope projection image of a horizontal brain section at the level of the VTA showing the schematic delineation of the medial (M) and lateral (L) parts of the VTA. Scale bar = 500 μm. (B–D) Confocal images of biocytin-filled neurons **(B)**, TH staining **(C)** and a merged image indicating that the recorded neuron was immunopositive for TH and thus identified as a putative DAergic neuron (upper arrow) or immunonegative for TH and thus identified as a putative non-DAergic neuron (lower arrow) **(D)**. Scale bar = 50 μm. **(E)** Representative APs of putative DAergic (left) and putative non-DAergic (right) VTA neurons showing differences in the peak to AHP minimum time (dashed lines). **(F)** Charts showing the AP peak to AHP time in the control (circles) and MS groups (triangles). The open symbols designate TH-positive putative DAergic neurons, and filled symbols designate TH-negative putative non-DAergic neurons. Note the lack of overlap between AP peak to AHP time values of TH-ir and TH-negative neurons in both groups. The group symbols and whiskers represent the means and SDs. The asterisks indicate statistical significance determined by one-way ANOVA (****$p < 0.0001$). Abbreviations: *CLi* caudal linear nucleus of the raphe, *fr* fasciculus retroflexus, *ml* medial lemniscus, *MT* medial terminal nucleus of the accessory optic tract, *PBP* parabrachial pigmented nucleus of the VTA, *rs* rubrospinal tract, *SNC* substantia nigra compact part, *vtgx* ventral tegmental decussation.

whether the fitted curves were different between groups. Further data analysis was performed using two-way repeated-measures ANOVA with current pulse amplitude as the first factor and treatment (control or MS) as the second. Cumulative inter-event interval and amplitude distributions of sEPSC were compared using the Kolmogorov–Smirnov (KS) test. For Sholl analysis data, two-way repeated-measures ANOVA with radial distance from the soma as the first factor and treatment (control or MS) as the second factor was used. In comparisons of control M and L dendritic tree complexity, the second factor was cell location (M or L). Sidak's test (electrophysiological data) or uncorrected Fisher's LSD test (morphological data) was used for post hoc comparisons between groups. To analyse spine head diameter the Mann-Whitney test was performed. For all data sets, a p value of less than 0.05 was considered statistically significant. The data are presented as the means ± SDs.

3. Results

3.1. Immunohistochemical and electrophysiological identification of VTA neurons

Whole-cell recordings and subsequent analysis of APs of cells from the control group revealed that VTA TH-ir neurons exhibited a significantly longer AP peak to AHP time (range: 4.68–22.08 m s, mean: 11.04 ± 4.14 m s, n = 57) than TH-negative neurons (range: 0.90–2.77 m s, mean: 1.70 ± 0.5 m s, n = 14, Fig. 1E) ($p < 0.0001$). Similarly, MS TH-ir cells were characterized by a significantly longer AP peak to AHP time (range: 4.80–20.63 m s, mean: 10.20 ± 3.62 m s, n = 55) than MS TH-negative neurons (range: 0.84–2.96 m s, mean: 2.0 ± 0.62 m s, n = 11) ($p < 0.0001$). Importantly, there was no AP peak to AHP time overlap between TH-ir- and TH-negative neurons in either group (Fig. 1F). At the same time, there were no differences in AP peak to AHP time between control TH-ir and MS TH-ir cells ($p > 0.9999$) or between control TH-negative and MS TH-negative cells ($p > 0.9999$, Fig. 1F). The difference in AP peak to AHP time between TH-ir- and TH-negative neurons allowed us to assign a cell type (putative DAergic vs. non-DAergic) to neurons not identified by biocytin and TH immunoreactivity. Overall, a total of 147 (77 from the control and 70 from the MS group) putative

DAergic neurons (106 neurons assigned to the putative DAergic group on the basis of staining and 41 neurons assigned to the putative DAergic group on the basis of electrophysiological characteristics) and 56 (29 from the control and 27 from the MS group) putative non-DAergic neurons (25 neurons assigned to the putative non-DAergic group on the basis of staining and 31 neurons assigned to the putative non-DAergic group on the basis of electrophysiological characteristics) were included in further analyses.

3.2. Maternal separation does not alter majority of the passive membrane properties of VTA putative DAergic neurons

The membrane properties of VTA putative DAergic cells in the medial VTA (M VTA) and lateral VTA (L VTA) were examined in current-clamp mode and compared (Table 1). ANOVA revealed that the capacitance and time constant were not affected by MS in putative DAergic neurons in any of the analysed parts of the VTA. At the same time MS caused an increase in the membrane resistance of examined neurons. Among examined active membrane properties, a decrease in rheobase value was observed after MS in the medial VTA. Moreover, ANOVA showed a significant treatment vs. location interaction in the sag value, however post-hoc test results did not reach statistical significance (Table 1).

3.2.1. Maternal separation increases the excitability of a subpopulation of VTA putative DAergic neurons

Analysis of the number of evoked action potentials versus stimulus intensity showed that sigmoidal curves best fit the pattern of voltage responses of examined neurons (Fig. 2, Table 1). Two-way repeated-measures ANOVA and subsequent post-hoc tests did not reveal differences between the control L VTA DAergic and MS L VTA DAergic groups, indicating a lack of influence of MS on the excitability of putative DAergic neurons in the lateral VTA (Fig. 2A and B, Table 1). However, it should be noted that the analysis of action potential properties of control L VTA DAergic and MS L VTA DAergic neurons showed that maternal deprivation increased the AP threshold (Table 1).

Interestingly, we found that MS strongly increased the excitability of

Table 1

Electrophysiological properties of putative DAergic VTA neurons (in brackets - number of tested neurons).

Parameter		Mean ± SD (n)		Two-way ANOVA effects (p values)			Post hoc (Holm-Sidak's test)	
		Control	MS	Treatment	M/L location	Interaction	L	M
Membrane properties DA neurons								
Resistance [MΩ]	L	310.70 ± 106.58 (60)	324.23 ± 118.68 (52)	0.03*	<0.0001****	0.12	–	–
	M	439.30 ± 143.1 (25)	525.86 ± 219.97 (26)					
TaU [ms]	L	36.37 ± 12 (60)	37.28 ± 10.46 (52)	0.35	0.32	0.62	–	–
	M	37.43 ± 8.75 (25)	40.36 ± 17.28 (26)					
Ce [pF]	L	120.25 ± 33.46 (60)	122.40 ± 35.33 (52)	0.28	<0.0001****	0.14	–	–
	M	91.78 ± 26.9 (25)	77.79 ± 27.45 (26)					
Rheobase [nA]	L	0.21 ± 0.08 (59)	0.23 ± 0.07 (50)	0.22	0.0003***	0.003**	0.12	0.03*
	M	0.29 ± 0.1 (25)	0.24 ± 0.1 (25)					
Sag [mV]	L	−18.51 ± 7.67 (60)	−20.06 ± 8.72 (52)	0.17	0.007**	0.02*	0.40	0.05
	M	−26.78 ± 9.9 (25)	−20.75 ± 14.07 (26)					
Action Potential shape DA neurons								
Time to first spike [ms]	L	395.7 ± 86.36 (56)	414.2 ± 73.9 (47)	0.54	0.05	0.46	–	–
	M	432.6 ± 47.51 (19)	430.8 ± 37.83 (20)					
Threshold [mV]	L	−45.19 ± 8.05 (60)	−41.36 ± 7.42 (50)	0.02*	0.007**	0.06	–	–
	M	−38.61 ± 5.25 (25)	−40.40 ± 6.65 (25)					
Amplitude [mV]	L	69.13 ± 7.78 (57)	66.35 ± 7.28 (49)	0.33	0.003**	0.25	–	–
	M	63.72 ± 5.71 (23)	63.94 ± 8.42 (24)					
10–90 Rise [ms]	L	0.49 ± 0.07 (57)	0.53 ± 0.14 (49)	0.32	0.35	0.39	–	–
	M	0.53 ± 0.14 (23)	0.53 ± 0.09 (22)					
Half width [ms]	L	1.27 ± 0.3 (57)	1.40 ± 0.35 (48)	0.16	0.06	0.36	–	–
	M	1.43 ± 0.29 (23)	1.46 ± 0.34 (24)					
AHP minimum [mV]	L	−68.55 ± 3.92 (57)	−67.56 ± 3.85 (49)	0.17	0.16	0.96	–	–
	M	−67.53 ± 5.42 (23)	−66.47 ± 4.51 (24)					
Peak to AHP [ms]	L	11.78 ± 4.33 (54)	11.30 ± 3.39 (46)	0.79	<0.0001****	0.62	–	–
	M	8.08 ± 2.02 (21)	8.22 ± 2.4 (23)					
Excitability DA neurons								
Sigmoid curve slope	L	0.15 ± 0.01 (55)	0.15 ± 0.007 (46)	0.05	0.003**	0.04*	0.99	0.04*
	M	0.006 ± 0.008 (15)	0.013 ± 0.009 (20)					
sEPSCs DA neurons								
Amplitude [pA]	L	13.18 ± 2.4 (38)	14.05 ± 2.69 (29)	0.007**	0.03*	0.28	–	–
	M	11.44 ± 1.9 (17)	13.45 ± 2.96 (19)					
Frequency [Hz]	L	0.60 ± 0.43 (38)	0.90 ± 0.59 (29)	<0.0001****	0.08	0.17	–	–
	M	0.26 ± 0.16 (17)	0.86 ± 0.7 (19)					
Rise time 10-90	L	2.05 ± 0.18 (38)	2.04 ± 0.26 (27)	0.69	0.27	0.69	–	–
	M	2.00 ± 0.03 (17)	1.96 ± 0.17 (18)					
Decay constant (Tau)	L	4.62 ± 1.26 (36)	4.76 ± 1.71 (27)	0.57	0.58	0.33	–	–
	M	5.15 ± 1.35 (15)	4.61 ± 2.22 (19)					

DAergic neurons in the medial part of the VTA. Analysis of the pattern of voltage response versus injected current showed that the sigmoidal curve fitted to the data from MS M VTA DAergic neurons had an elevated slope in comparison with the flattened slope of the curve fitted to the control M VTA DAergic neuron data, and the difference was statistically significant (Fig. 2 C, D, Table 1). Accompanying two-way repeated-measures ANOVA revealed that MS remarkably altered neuronal excitability in the medial VTA. Depolarizing current steps in the range of 0.09–0.14 nA evoked a significantly higher number of action potentials in MS M VTA DAergic neurons than in control M VTA DAergic neurons (p = 0.017 – p < 0.0001, Fig. 2D). At the same time, MS did not influence action potential shape of M VTA DAergic neurons; however, we found that, in line with recorded increased excitability, rheobase was significantly reduced and AP threshold was decreased by MS in M VTA DAergic neurons (Table 1).

3.2.2. Maternal separation enhances excitatory synaptic currents in VTA putative DAergic neurons

To investigate whether maternal separation modifies excitatory synaptic inputs to VTA putative DAergic neurons, sEPSCs were recorded in voltage-clamp mode at −70 mV (Fig. 3A and B). Under these conditions, only EPSCs were visible, and the dependence of these currents on glutamatergic transmission was confirmed by their abolishment in the presence of glutamate ionotropic receptor antagonists (50 μM D-2-amino-5-phosphonopentanoic acid (D-AP5) and 10 μM 6-cyano-7-nitro-quinoxaline-2,3-dione (CNQX). ANOVA revealed that MS significantly altered the mean amplitude of sEPSC recorded from putative DAergic neurons, regardless of the location of the recordings (Fig. 3 C, Table 1).

However, the difference in the mean sEPSC amplitude between MS and control groups in the lateral VTA was small and the cumulative frequency distribution of sEPSCs amplitudes in the lateral VTA was not different between the groups (p = 0.3, KS test, Fig. 3 D). On the other hand, MS altered the cumulative frequency distribution of sEPSCs amplitudes in the medial VTA (p = 0.04, KS test). Plots of cumulative data from MS M VTA DAergic neurons were shifted to the right in relation to control (Fig. 3E).

The mean frequency of sEPSCs recorded from cells located in both the lateral and medial parts of the VTA was markedly increased by maternal separation (Fig. 3 F, Table 1). Also, cumulative frequency distributions of sEPSCs inter-event intervals from MS L VTA DAergic and MS M VTA DAergic were significantly different from controls (p < 0.0001, KS test L VTA; p < 0.0001 KS test M VTA). Plots of cumulative data from both MS L VTA DAergic and MS M VTA DAergic neurons were shifted to the left (Fig. 3 G, H). At the same time, no significant changes were detected in sEPSC kinetics. Maternal separation did not alter either the rise time or decay time constant of sEPSCs (Table 1).

3.3. Maternal separation does not modify the membrane properties of VTA putative non-DAergic neurons

Membrane properties were analysed from voltage-current relationships and responses to current ramp stimuli. MS exerted no influence on membrane resistance, time constant, capacitance or voltage sag in either lateral or medial VTA non-DAergic neurons (Supplementary Tab. 1).
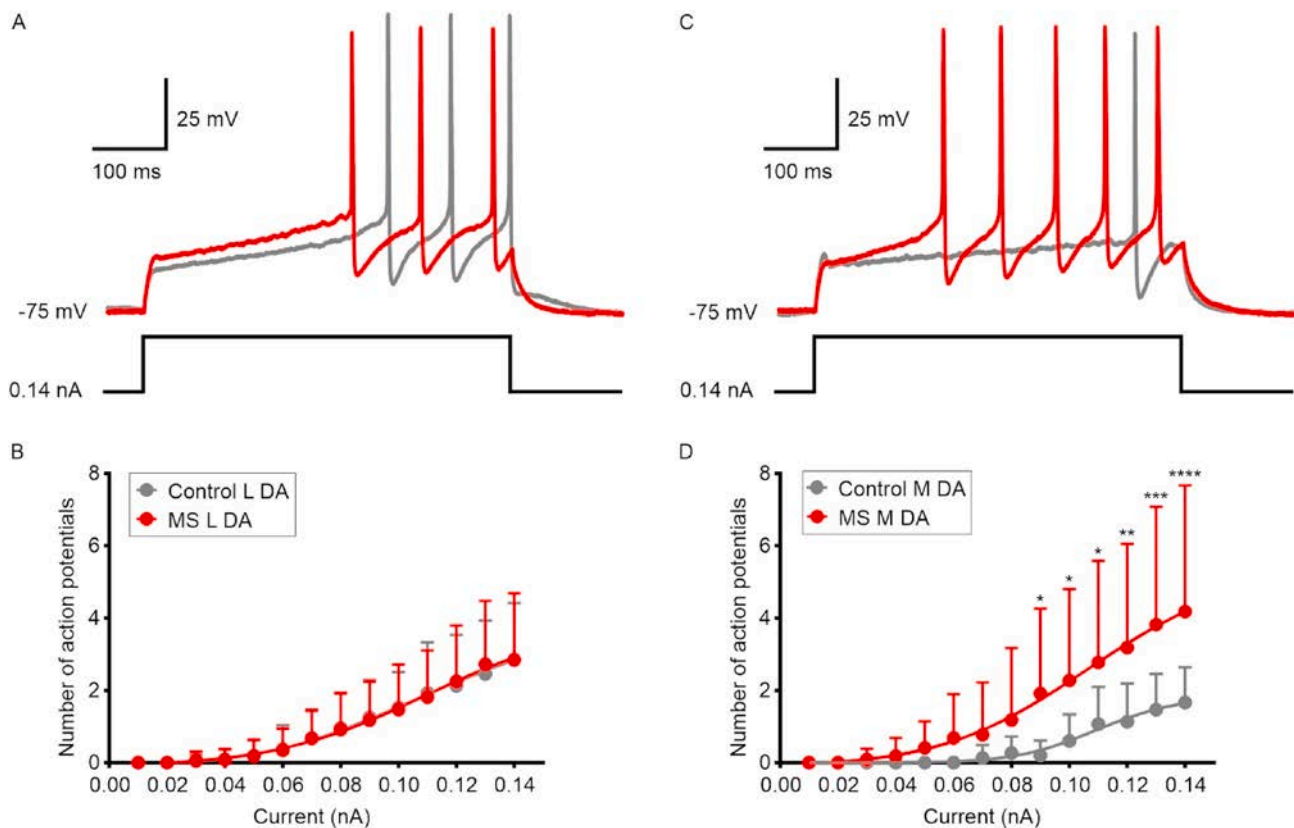
Fig. 2. Maternal separation (MS) increases the excitability of putative DAergic neurons in the medial part of the VTA. **(A)** The current-step stimulation protocol (bottom) and representative voltage responses of lateral (L) VTA putative DAergic neurons (top) from the control (grey) and MS (red) groups. **(B)** Line chart showing the number of evoked action potentials versus stimulus intensity illustrating the lack of influence of MS on the excitability of putative DAergic neurons in the lateral part of the VTA. **(C)** Current-step stimulation protocol (bottom) and representative voltage responses of medial (M) VTA putative DAergic neurons (top) from the control (grey) and MS (red) groups. **(D)** Line chart showing increased excitability of putative DAergic neurons of the MS group in the medial part of the VTA. The group symbols and whiskers represent the means and SDs. The lines connect consecutive means. The asterisks indicate statistical significance by two-way ANOVA (p = 0.027 – p < 0.0001) (*p < 0.05, **p < 0.01, ***p < 0.001, ****p < 0.0001). (For interpretation of the references to color in this figure legend, the reader is referred to the Web version of this article.)

3.3.1. Maternal separation does not alter the excitability of VTA non-DAergic neurons

Analysis of the number of action potentials versus injected current showed that the pattern of voltage responses in control non-DAergic and MS non-DAergic neurons could be fitted by linear regression. The slope of the line representing the data from MS L VTA non-DAergic neurons was slightly smaller (Fig. 4B) than that of the data from control L VTA non-DAergic neurons, but the difference was not statistically significant. Similarly, there were no differences between the slopes of the lines fitted to the data from control M VTA non-DAergic and MS M VTA non-DAergic neurons (Fig. 4D, Supplementary Tab. 1). Subsequent two-way repeated-measures ANOVA comparing the number of spikes evoked in response to current stimulus steps showed no differences between groups (main effect of treatment F1,40 = 0.796, p = 0.378).

Analysis of the action potential shape of control L VTA non-DAergic and MS L VTA non-DAergic neurons as well as control M VTA non-DAergic and MS M VTA non-DAergic neurons showed that maternal separation had no influence on AP threshold, 10–90% rise time, amplitude, half width, AHP minimum or AP peak to AHP time (Supplementary Tab. 1).

3.3.2. Maternal separation does not modify excitatory synaptic transmission in VTA non-DAergic neurons

To determine whether maternal separation changes excitatory inputs to non-DAergic neurons, we measured both the amplitude and frequency of sEPSCs and sEPSC kinetics (Fig. 5). We observed that MS had no effect on the parameters of sEPSCs in non-DAergic neurons located in both the

lateral and medial parts of the VTA. Analysis of data obtained from control non-DAergic and MS non-DAergic neurons showed that there were no changes in the mean amplitude (Fig. 5C, G) or mean frequency (Fig. 5 E, I) of recorded sEPSCs. Similarly, no differences were detected in cumulative data distributions of sEPSC amplitudes (p > 0.9999, KS test L VTA; p = 0.72, KS test M VTA) and inter-event intervals (p = 0.57, KS test L VTA; p = 0.44, KS test M VTA) (Fig. 5 D, H, F, J). No significant changes were observed in the sEPSC kinetics of VTA non-DAergic neurons. Maternal separation did not alter either the rise time or decay time constant of sEPSCs (Supplementary Tab. 1).

3.4. MS has little effect on the dendritic tree structure of morphologically divergent medial and lateral VTA putative DAergic neurons

3D reconstructions of the dendritic trees of biocytin-filled neurons were subjected to Sholl analysis (Fig. 6, Supplementary Tables 5 and 6). Two-way ANOVA revealed that MS had no effect on the overall dendritic tree complexity of neither L nor M VTA DAergic neurons (Fig. 6A, Supplementary Tables 5 and 6). Amongst all the morphological features describing dendritic tree that were tested (the total dendritic length, branch order, the number of primary dendrites, bifurcations and branches and the number of dendritic tips), only the number of dendritic tips was affected by MS. The conducted analysis showed that the number of dendritic tips was increased in the medial but not the lateral VTA in the MS group (Fig. 6D, Supplementary Tab. 2).

Although we did not detect an influence of MS on the dendritic tree structure in either the medial or lateral part of the VTA, we observed that
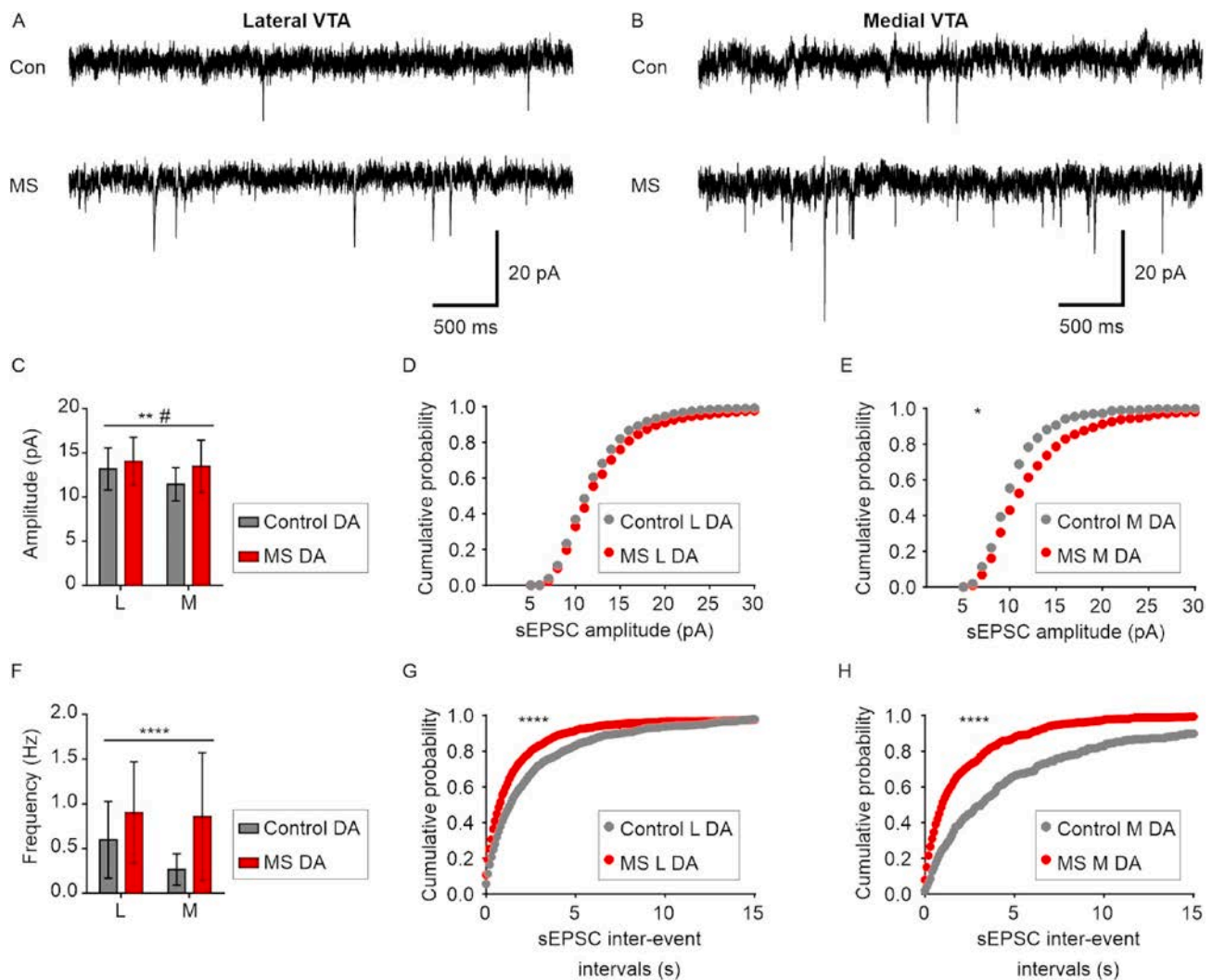
Fig. 3. Maternal separation (MS) enhances excitatory synaptic inputs to VTA putative DAergic neurons. **(A, B)** Representative traces of spontaneous synaptic events recorded from lateral **(A)** and medial **(B)** VTA putative DAergic neurons from the control (upper) and MS (bottom) groups in voltage clamp mode at a holding potential of −70 mV. **(C)** Chart showing the spontaneous postsynaptic currents (sEPSCs) amplitudes recorded from lateral (L) and medial (M) VTA putative DAergic neurons in the control and MS groups, showing significant differences between experimental groups (MS and control, marked with asterisks) and between location of the recordings (marked with hash). **(D)** Unchanged cumulative frequency distribution of sEPSCs amplitudes recorded from lateral VTA DAergic neurons. **(E)** Cumulative distribution of sEPSC amplitudes recorded from medial VTA DAergic neurons, shifted to the right (higher values) in the MS group. **(F)** Chart showing the spontaneous postsynaptic currents (sEPSCs) frequencies recorded from lateral (L) and medial (M) VTA putative DAergic neurons in the control and MS groups, showing significant differences between experimental groups (MS and control, marked with asterisks). **(G)** Cumulative distribution of the sEPSCs inter-event intervals, recorded from lateral VTA DAergic neurons, shifted to the left (shorter values) in MS group. **(H)** Cumulative distribution of sEPSC inter-event intervals, shifted to the left (shorter intervals) in MS group. The group symbols and whiskers represent the means and SDs. The asterisks and hashes indicate statistical significance determined by two-way ANOVA in **C, F** and KS test in **D, E, G, H** ($*p < 0.05$, $**p < 0.01$, $****p < 0, 0001$).

control neurons from the lateral region had larger and more complex dendritic trees than in medial VTA. A significant M/L location effect was showed by the two-way ANOVA in three morphological parameters: the number of primary dendrites, bifurcations and branches, accompanied by a tendency toward significance (p value = 0.05) in the total dendritic length (Fig. 6D, Supplementary Tab. 2). Two-way ANOVA and subsequent post hoc tests of data obtained through Sholl analysis of the putative DAergic L and M VTA neurons from control animals, confirmed pronounced dissimilarity in their dendritic tree complexity (Fig. 6A, bottom, Supplementary Tab. 7). Significant differences in the number of intersections on proximal and medial dendrites (located within one third of the radial distance from the soma to the outermost dendritic tips or in its middle area, respectively) were found at distances of 70–120 and 140 μm from the soma (Fig. 6A, bottom, Supplementary Tab. 7).

3.5. MS does not change the dendritic spine density of VTA putative DAergic neurons but affects spine head diameter

Two-way ANOVA of the spine density of putative DAergic neurons did not reveal any differences based on the region of the VTA (M or L), a potential influence of MS or an interaction between both factors (Fig. 7, Supplementary Tab. 3).

However, MS induced a statistically significant increase in the diameter of spine heads on putative DAergic neurons in the lateral VTA, and this effect was specific to spines on first and second order dendrites (Fig. 7B, Supplementary Tab. 4). There were no significant differences in the diameter of spine heads on putative DAergic neurons in the medial VTA (Fig. 7B, Supplementary Tab. 4).
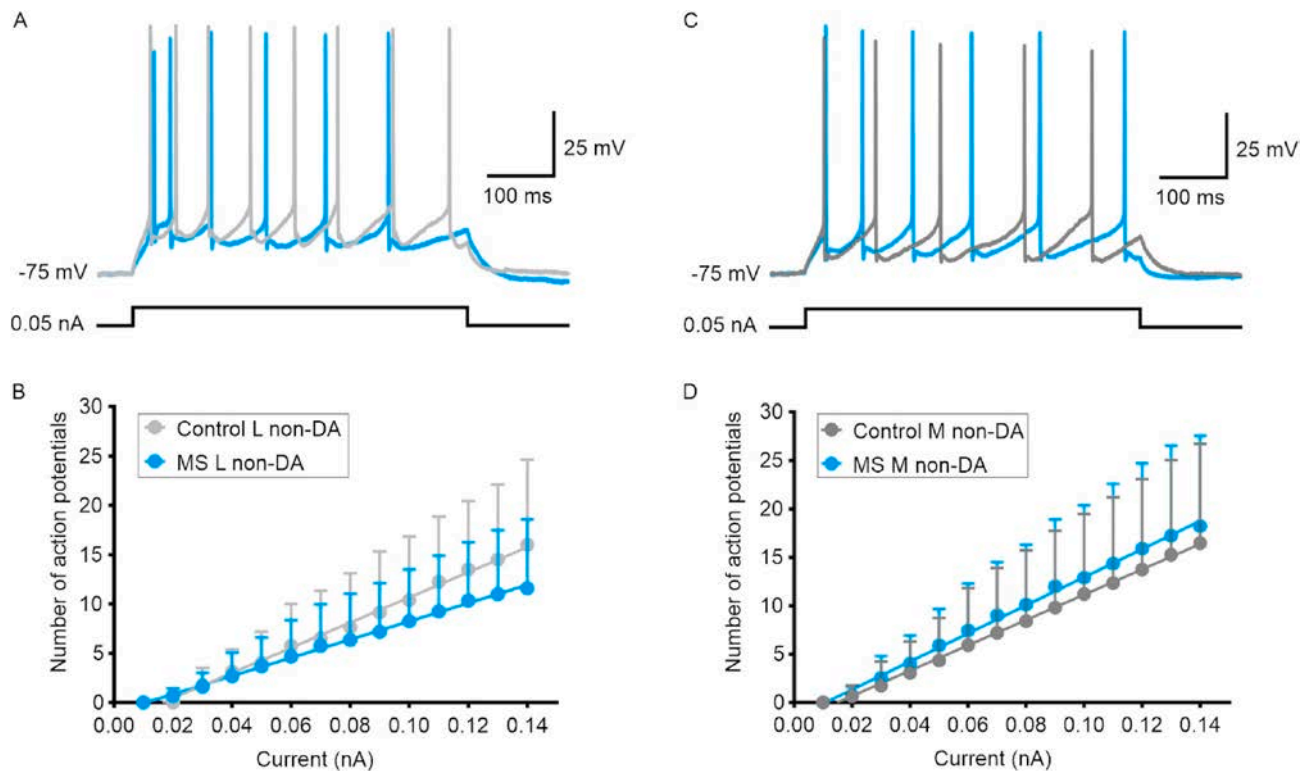
Fig. 4. Maternal separation (MS) does not alter the excitability of VTA putative non-DAergic neurons. **(A)** The current-step stimulation protocol (bottom) and representative voltage responses of lateral (L) VTA putative non-DAergic neurons (top) from the control (grey) and MS (blue) groups. **(B)** Line chart showing the number of evoked action potentials versus stimulus intensity illustrating the lack of influence of MS on the excitability of putative non-DAergic neurons in the lateral part of the VTA. **(C)** The current-step stimulation protocol (bottom) and representative voltage responses of medial (M) VTA putative non-DAergic neurons (top) from the control (grey) and MS (blue) groups. **(D)** Line chart showing the lack of influence of MS on the excitability of putative non-DAergic neurons in the medial part of the VTA. The group symbols and whiskers represent the means and SDs. The lines connect consecutive means. (For interpretation of the references to color in this figure legend, the reader is referred to the Web version of this article.)

3.6. MS causes an increase in basal serum corticosterone and ACTH levels

To verify the influence of MS on basal stress hormone levels, corticosterone and ACTH blood plasma levels in adolescent female rats were determined. MS treatment caused a significant increase in both corticosterone (139.9 ng/ml in the control vs. 178.9 ng/ml in the MS group, Mann-Whitney test, p = 0.009, Fig. 8A) and ACTH (359.5 ng/ml in the control vs. 547.6 ng/ml in the MS group, Mann-Whitney test, p = 0.009, Fig. 8B).

4. Discussion

Here, we provide a detailed characterization of the long-term effects of maternal separation (MS) on the electrophysiology and structure of VTA neurons in adolescent female rats. We described MS-induced increase in excitability of putative DAergic neurons in the medial but not lateral part of the VTA. Moreover, we found an enhancement of excitatory synaptic transmission in both examined parts of the VTA. Furthermore, we demonstrated that the electrophysiological properties of putative non-DAergic neurons remained unchanged. We also showed that altered electrophysiology of putative DAergic VTA neurons was accompanied by small changes in the anatomy of these cells and an increase in the diameter of spine heads on putative DAergic neurons in the lateral VTA. Finally, we reported MS-induced increases in basal plasma ACTH and corticosterone levels.

4.1. Identification of VTA neurons

In the present study, to characterize putative DAergic neurons, we used tyrosine hydroxylase (TH) staining, which allows post hoc identification of DAergic neurons filled with biocytin during recording. Because anti-biocytin staining was not always successful, we used electrophysiological characteristics to assign recorded neurons to either the putative DAergic or non-DAergic group. Within the VTA, DAergic neurons are intermingled with those that synthesize GABA or/and glutamate, and some DAergic cells co-release glutamate and/or GABA (reviewed in Morales and Margolis, 2017). The presence of the Ih current mediated by hyperpolarization-activated cyclic nucleotide-regulated cation (HCN) channels, low-frequency pacemaker activity, broad action potentials or sensitivity to D2 receptor activation, have previously been used to identify DAergic neurons. However, more recent studies have shown that none of these criteria allow unequivocal determination of the neurochemical character of VTA neurons ex vivo (Margolis et al., 2006; reviewed in Ungless and Grace, 2012; Lammel et al., 2014). In the current study, we showed that the AP peak to AHP trough time of TH-positive cells was longer than that of TH-negative neurons, and that the values of this parameter did not overlap between groups what allowed us to assign recorded neurons to the putative DAergic or putative non-DAergic group. Notably, this observation was valid regardless of the recording site (medial or lateral VTA). Our observations are in agreement with extracellular AP recordings from single VTA neurons in anaesthetised rats (Ungless et al., 2004). In that study, DAergic and non-DAergic AP widths were shown to overlap to some extent, whereas in our ex vivo recordings, they did not. Although our results did not allow for the characterization of recorded neurons as GABA- or glutamate-synthesizing, they provide a useful tool for the classification of VTA neurons in ex vivo preparations as putatively DAergic, regardless of the VTA subregion location.
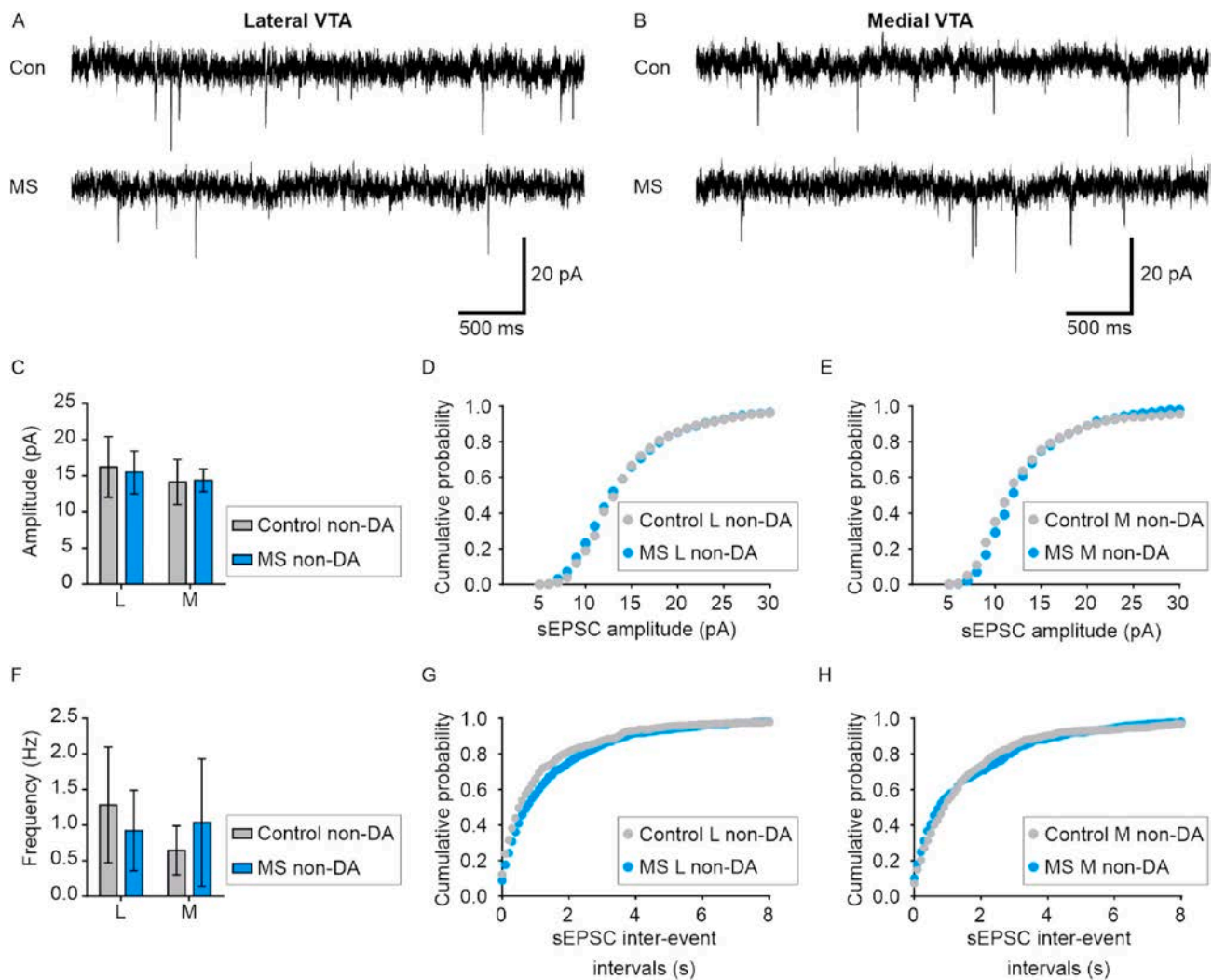
Fig. 5. Maternal separation (MS) does not influence excitatory synaptic inputs to VTA non-DAergic neurons. **(A, B)** Representative traces of spontaneous synaptic events recorded from lateral **(A)** and medial **(B)** VTA putative non-DAergic neurons from the control (upper) and MS (bottom) groups in the voltage clamp mode at a holding potential of −70 mV. **(C)** Charts showing lack of differences in amplitudes of the spontaneous postsynaptic currents (sEPSC) recorded from lateral and medial VTA putative non-DAergic neurons in the control and MS groups. **(D, E)** Unchanged cumulative frequency distribution of sEPSCs amplitudes recorded from lateral **(D)** and medial **(E)** non-DAergic VTA neurons. **(F)** Charts showing the frequency of sEPSCs, unaffected by MS, recorded from lateral and medial VTA putative non-DAergic neurons. **(G, H)** Cumulative frequency distribution of sEPSC inter-event intervals, unchanged by MS, recorded from lateral **(G)** and medial **(H)** putative non-DAergic VTA neurons. The group symbols and whiskers represent the means and SDs.

4.2. MS-induced changes in VTA neuronal excitability

MS-induced changes in properties of VTA neurons, described in the current paper, concern a specific stage in the development of the dopaminergic system. During adolescence dopaminergic pathways undergo specific alterations including an increase in dopamine concentration and fiber density in the PFC, an increase of dopamine turnover in striatum and pruning of DAergic receptors. Among the consequences of this substantial reorganization, increased risk taking, drug use, intensifications of social interactions and elevations in novelty-seeking behaviors can be indicated (reviewed in Spear, 2000). At the same time it was shown that a history of early life stress further increases the likelihood of substance abuse and engaging in risky behaviours, the phenomena largely dependent on the activity of the dopaminergic system (Andersen, 2019; Fergusson et al., 2000; Kessler et al., 1997). We showed that MS, an animal model of early life stress, caused an increase in the intrinsic excitability of DAergic neurons in the medial part of the VTA. These results reveal a possible neuronal mechanism of the activational influence of early life adversities on the DAergic system in rodents.

It has been shown that rats that undergo the MS procedure during early stages of development (sex not specified) are hyperactive in a novel setting and more sensitive to cocaine in adulthood (Meaney et al., 2002; Brake et al., 2004). Notably, these observations are accompanied by MS-induced increase in acute stress-evoked DA levels in the striatum. Increased basal activity of the mesocortical and mesolimbic DAergic systems (indicated by a higher DA level) has also been observed after MS in male adolescent degus (Jezierski et al., 2007) and adult rats of both sexes (Matthews et al., 2001). MS-induced behavioral alterations and changes in the DA level might be related to increased excitability of a subpopulation of putative DAergic neurons, as described in the present study. Importantly, we showed that the properties of putative non-DAergic neurons remained unchanged after MS. These observations indicate particular sensitivity of DAergic neurons to stress during periods of development.

In the current study we revealed that MS-induced changes in excitability are restricted to the medial parts of the VTA. Observed selective susceptibility of different VTA parts to MS, may be related to their distinct reactivity to stress. It was shown that while lateral VTA neurons are mainly inhibited during acute stress, medially located putative
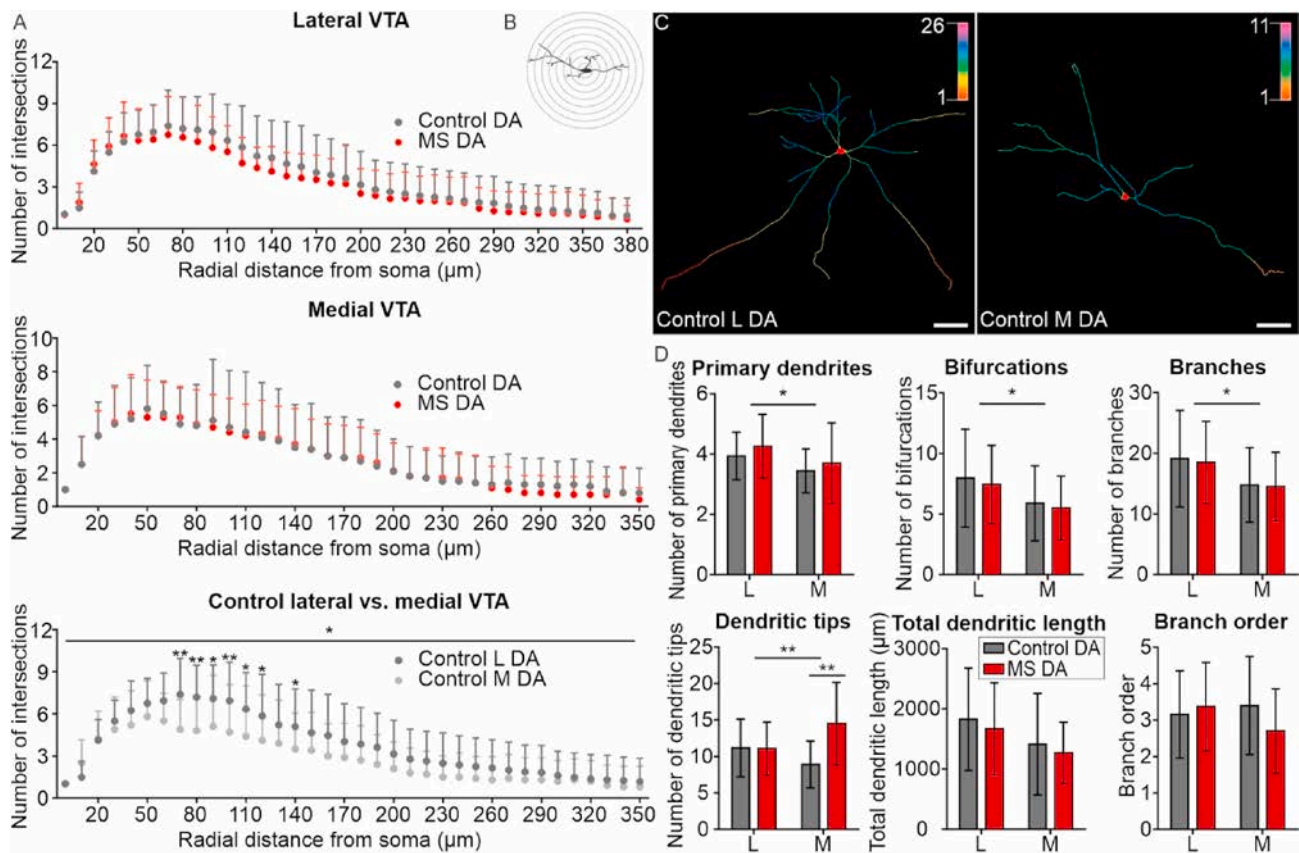
Fig. 6. Dendritic tree morphology differs between putative DAergic neurons in the medial and lateral parts of the VTA, with no profound effect of maternal separation (MS). **(A)** Sholl analysis of 3D-reconstructed control and MS putative DAergic neurons showing that MS had no effect on the dendritic complexity in both the lateral (L) and medial (M) parts of the VTA (top and middle, respectively); medial and lateral VTA control putative DAergic neurons exhibited profound differences in the structure of their proximal and middle dendritic tree compartment, where significantly more intersections were discovered in the L VTA (bottom). The symbols indicate statistical significance by two-way RM ANOVA and post hoc uncorrected Fisher's LSD test (*p < 0.05, **p < 0.01, see Supplementary Tables 5–7). **(B)** Schematic representation of the Sholl analysis method. **(C)** Representative images of skeletal 3D reconstructions of control L (left) and M (right) VTA putative DAergic neurons, color-coded to indicate the number of dendrites intersecting with Sholl spheres. Scale bar = 100 μm. **(D)** Graphs showing dendritic tree parameters of control and MS putative DAergic neurons in the L and M VTA, which were compared by two-way ANOVA and post hoc uncorrected Fisher's LSD test (see Supplementary Table 2). Note that MS affected the number of dendritic tips in the M but not L VTA (bottom, left). L VTA putative DAergic neurons had more primary dendrites, bifurcations and branches (top, left, middle and right, respectively). The group symbols and whiskers represent the means and SDs. The asterisks indicate statistical significance (*p < 0.05, **p < 0.01). (For interpretation of the references to color in this figure legend, the reader is referred to the Web version of this article.)

DAergic VTA neurons are phasically activated by stressor exposure (reviewed in Douma and de Kloet, 2020). Moreover, DAergic neurons of the medial VTA area are characterized by particularly high expression of glucocorticoid receptors (Harfstrand et al., 1986), which potentially makes them more sensitive to stress.

Findings from recent studies on male rodents showed that different VTA subnuclei play distinct roles in reward, motivation, aversion and learning (Lammel et al., 2011, 2012; 2014; Stamatakis et al., 2013). Diversity in function of different VTA areas is reflected in specific anatomy of VTA inputs and outputs. While medial part of the VTA projects predominantly to the medial prefrontal cortex (mPFC), baso-lateral amygdala, nucleus accumbens (NAc) core and NAc medial shell, DAergic projections to the NAc lateral shell originate from the lateral VTA (reviewed in Juarez and Han, 2016; Lammel et al., 2012, 2014). Neurons innervating the mPFC and NAc medial shell have been shown to encode aversion, whereas those projecting to the NAc lateral shell have been characterized as reward-encoding (Lammel et al., 2012; de Jong et al., 2019). Additionally, afferent projections to specific parts of the VTA differ in terms of their sources and functionalities. Neurons in the medial, but not the lateral VTA, receive dense innervation from the lateral habenula (LHb) (Lammel et al., 2012), which participates in aversion and the absence of an expected reward signalling (Hikosaka,

2010). Therefore, MS-induced increased excitability of medial VTA neurons, described in the current study, may underlby augmented vulnerability to stress induced behavioral disturbances in individuals who experienced early life maltreatment. Moreover, the differences in the morphology of putative DAergic neurons localized in the medial and lateral VTA, with lateral DAergic neurons having more complex dendritic trees, as well as previously reported latero-medial gradient of the two morphological cell types in the VTA (Phillipson, 1979; Sarti et al., 2007), further strengthen the distinctiveness of the different parts of the VTA.

4.3. MS impact on the excitatory transmission in the VTA

In the current study we found that MS strengthened glutamatergic inputs to the VTA. In putative DAergic neurons of both examined parts of the VTA, an increased mean amplitude and frequency of sEPSCs were observed, which is indicative of both pre- and postsynaptic effects of MS. In the medial VTA, observed changes in the mean amplitude and frequency of recorded sEPSC were accompanied by marked shifts in cumulative frequency distributions towards larger amplitudes and shorter inter-event intervals. In the lateral VTA, where MS-induced changes in the mean amplitude and frequency of EPSCs were smaller, only the
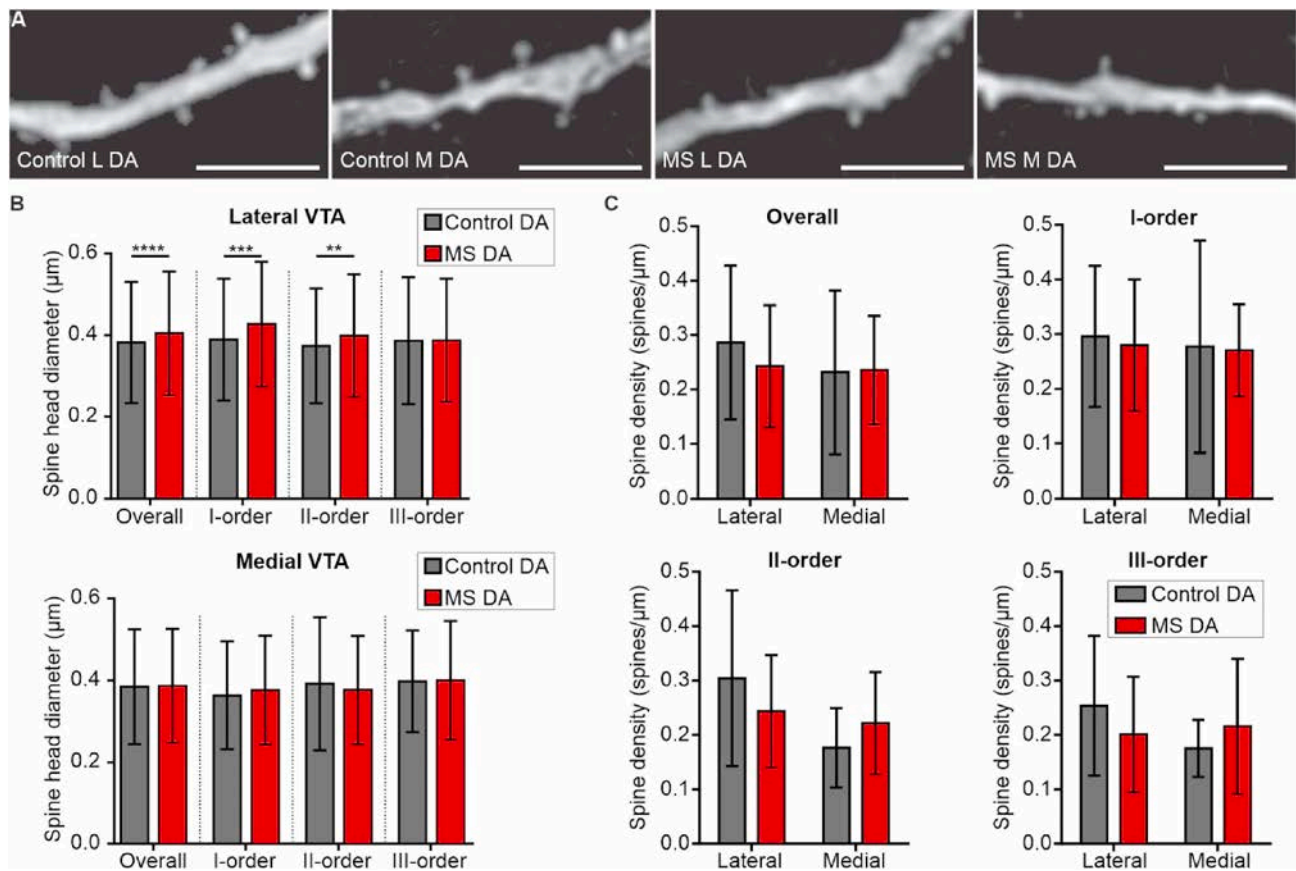
Fig. 7. Maternal separation (MS) does not change the dendritic spine density but modifies the diameter of spine heads on VTA putative DAergic neurons. **(A)** Representative high-power confocal images showing dendritic segments of VTA putative DAergic neurons with dendritic spines from each group. Scale bar = 5 μm. **(B)** Graphs showing increased diameter of dendritic spine heads on putative DAergic neurons in the lateral (top) and unchanged diameter in the medial (bottom) VTA. The symbols indicate statistical significance by the Mann-Whitney test (see Supplementary Table 4) (**$p < 0.01$, ***$p < 0.001$, ****$p < 0.0001$). **(C)** Graphs showing the overall and order-specific dendritic spine density of lateral and medial VTA putative DAergic neurons, with no significant differences between these two regions and no MS effect (as indicated by two-way ANOVA, see Supplementary Table 3). The group symbols and whiskers represent the means and SDs.
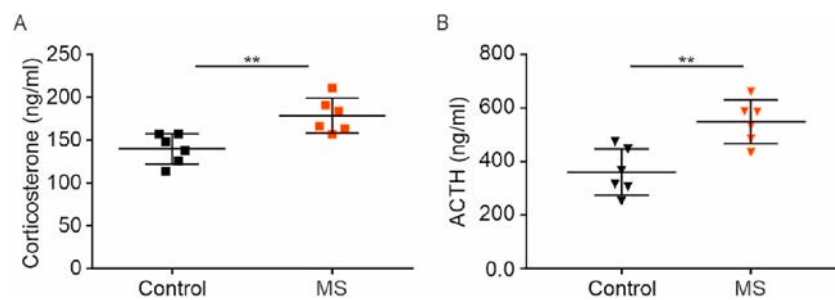

Fig. 8. Maternal separation (MS) influences corticosterone and ACTH levels. **(A)** Increased corticosterone and **(B)** ACTH concentrations in the plasma of MS rats (n = 6) in relation to control (n = 6). The group symbols and whiskers represent the means and SDs. The asterisks indicate statistical significance by the Mann-Whitney test (**$p < 0.01$).

cumulative distribution of inter-event intervals was significantly shifted toward shorter values, which suggests different mechanism of the influence of MS on excitatory inputs in both parts of the VTA. Importantly, functional diversity of the glutamatergic innervation of the VTA has been described. Glutamatergic fibres originating in the dorsal raphe, found mainly in the lateral VTA, have been shown to promote reward, and glutamatergic inputs from the lateral hypothalamus, which mainly innervate the medial VTA, have been shown to mediate aversive behaviours (de Jong et al., 2019). Therefore, the MS-induced alterations in glutamatergic signalling in the VTA reported in the current study may be involved in changes in both reward and aversion processing during

adolescence. The mechanisms underlying different effect of MS on glutamatergic transmission in the medial and lateral VTA remain open for further investigation.

Although limited, other studies also showed an influence of a different kind of stress during the early developmental stage, on the electrophysiology of VTA neurons. It was shown that severe early life stress (24h of maternal deprivation on PND 9) does not alter glutamatergic synaptic transmission and plasticity of VTA neurons in PND 14–21 male rats, but induces long-term depression at GABAergic synapses onto VTA neurons ex vivo (Authement et al., 2015). At the same time, such severe maternal deprivation was reported to increase

spontaneous, putative DAergic, VTA neuronal activity and excitability in juvenile (PND 14–21) male rats, without affecting intrinsic excitability of these cells (Shepard et al., 2020). It should be pointed out, however, that putative DAergic neurons in that study were identified by the presence of the Ih current, the criterium that does not allow unequivocal determination of the neurochemical character of VTA neurons. It was also shown that in urethane anaesthetised male adult rats (PND 70–80), MS similar to that used in the current study, led to a decrease in firing rate and an increase in the variability of baseline discharge activity of VTA neurons (Masrouri et al., 2020). Although differences in the type of stressors, sex, and age of used animals do not allow for a direct comparison of results of these studies with the present data, altogether, these results indicate a strong influence of early life stress on the electrophysiological properties of VTA neurons that may constitute a possible neuronal mechanism of early life adversities induced malfunctioning of the reward system.

4.4. Dendritic morphology and spine density in VTA after MS

Neuronal activity may modify dendritic morphology and remodel dendritic spines (Nakahata and Yasuda, 2018). In the current study, we did not observe MS-induced changes in the dendritic morphology or spine density on VTA putative DAergic neurons despite significantly altered excitatory neurotransmission. At the same time, we observed an increase in the diameter of dendritic spine heads on lateral VTA DAergic neurons, a feature that has been positively correlated with synaptic activity (reviewed in Gipson and Olive, 2017). Therefore, morphological changes in dendritic spine head diameter may constitute an anatomical substrate of increased synaptic activity in lateral VTA dopaminergic neurons after MS stress. The lack of relationship between the spine density/spine head diameter and changes in the excitatory neurotransmission in the medial VTA may be related to MS-induced modification in neurotransmitter release probability (Fitzgerald et al., 1996; Sola et al., 2004), or to the increased number of glutamatergic shaft synapses, that coexist with dendritic spines on midbrain dopaminergic neurons dendrites (Jang et al., 2015). Finally, an increase in the number of dendritic tips in the medial VTA, observed in the current study, may also be related to the observed enhancement of synaptic activity in this part of nucleus.

To date, there are no data concerning the influence of MS on the dendritic tree morphology or spine density of DAergic neurons in the VTA. Though, the effects of MS on other parameters of rat VTA cells have been studied. In agreement with our results, indicating a lack of MS-induced changes in most of the morphological features tested, the VTA TH-immunoreactive cells' soma size was not affected by an MS protocol similar to ours in prepubertal, adolescent and adult Wistar rats of both sexes (Chocyk et al., 2011). According to the same study, MS elevated the number of these cells in young adult females, suggesting its influence on the expression of TH, an enzyme involved in dopamine turnover. Moreover, MS may influence the number of VTA cells, as both an increase (presumably of non-DAergic VTA neurons, according to authors; prepubertal, adolescent and adult male Wistar rats, MS during PND 1–14; Chocyk et al., 2015) and a decrease (mixed group of male and female adult Sprague-Dawley rats, MS during PND 2–21; Gondré-Lewis et al., 2016) in total number of VTA neurons was reported. The first of these studies also revealed no changes in the number of VTA neurons in female Wistar rats of respective developmental stages, subjected to MS, comparing to control (Chocyk et al., 2015). Taken together, these data strongly suggest that age, sex, genetic background and the MS procedure used in the experiment is of particular importance for the resultant effects.

4.5. Long-term effect of MS on the level of stress hormones

A history of abuse has been shown to be the strongest predictor of hyperresponsiveness of the HPA axis, as indicated by ACTH and cortisol

levels, to psychological stressors in adolescence and adulthood (Heim et al., 2002; Kuhlman et al., 2015, 2015a). We showed that in female rats MS induced an increase in the basal levels of serum ACTH and corticosterone. Importantly, glucocorticoids have been shown to increase the sensitivity of VTA DAergic neurons to drugs (reviewed in Piazza and Le Moal, 1998). Based on the results of the current study, we propose a possible causal link between exposure to early life stress and increased vulnerability to drug addiction in which early stress dysregulates the activity of the HPA axis and induces an elevation of the levels of the HPA hormones ACTH and corticosterone, a condition that lasts for weeks after stressor termination (present study; Jahng et al., 2010; Hori-i-Hayashi et al., 2013; Nishi et al., 2014; also note that the effect of MS on stress hormone levels strongly depends on the type, timing and duration of the stressor as well as the developmental stage of tested animals; see Table 1 in Rees et al., 2006). The consequences of elevated corticosterone levels include increases in glutamatergic signalling and the excitability of VTA DAergic neurons, as shown by Overton et al. (1996) and the current study.

5. Conclusions

In the rat model of maternal neglect used in the present study, animals underwent MS from the second PND to the 14th PND, a stress hyporesponsive period in rodents, and this period corresponds to the first year of life in human postnatal development (Gunnar and Donzella, 2002). Therefore, the obtained results may be comparable to changes in the brain caused by neglect experienced during the first year of a child's life that persist until adolescence, and these changes may underlie the increased susceptibility of individuals that were abused/neglected in early life, to psychopathologies and addictive substance abuse (reviewed in Gee and Casey, 2015). The described MS-induced changes concern females, and since there are sex differences in the effects of early-life stress on later drug-intake behavior in rodents, as well as in vulnerability to mental disorders and substance abuse among humans (reviewed in Forster et al., 2018), further studies on male rats should help to determine possible sex differences in the sensitivity of VTA DAergic neurons to early life stress. Importantly, understanding neuronal mechanisms underlying childhood maltreatment-evoked changes in brain reward centres may lead to improved treatments for substance abuse and mental disorders. Our study supports the idea that these treatments should rely on restoring the normal functioning of brain areas innervated by the medial VTA DAergic neurons rather than manipulating DAergic receptors or DA release in general.

CRediT authorship contribution statement

Jadwiga Spyrka: Investigation, Formal analysis, Visualization.

Anna Gugula: Investigation, Formal analysis, Visualization. **Agnieszka Rak:** Investigation, Formal analysis, Visualization. **Grzegorz Tylko:** Software, Formal analysis. **Grzegorz Hess:** Conceptualization, Supervision, Writing - original draft, Writing - review & editing. **Anna Blasiak:** Conceptualization, Supervision, Writing - original draft, Writing - review & editing.

Declaration of competing interest

The authors have no conflicts of interest to declare.

Appendix A. Supplementary data

Supplementary data to this article can be found online at https://doi.org/10.1016/j.ynstr.2020.100250.

References

Andersen, S.L., 2019. Stress, sensitive periods, and substance abuse. Neurobiol. Stress 10, 100140. https://doi.org/10.1016/j.ynstr.2018.100140.

Authement, M.E., Kodangattil, J.N., Gouty, S., Rusnak, M., Symes, A.J., Cox, B.M., Nugent, F.S., 2015. Histone deacetylase inhibition rescues maternal deprivation-induced GABAergic metaplasticity through restoration of AKAP signaling. Neuron 86, 1240–1252. https://doi.org/10.1016/j.neuron.2015.05.024.

Boecker, R., Holz, N.E., Buchmann, A.F., Blomeyer, D., Plichta, M.M., Wolf, I., et al., 2014. Impact of early life adversity on reward processing in young adults: EEG-fMRI results from a prospective study over 25 years. PloS One 9. https://doi.org/10.1371/journal.pone.0104185.

Bonapersona, V., Kentrop, J., Van Lissa, C.J., van der Veen, R., Joëls, M., Sarabdjitsingh, R.A., 2019. The behavioral phenotype of early life adversity: a 3-level meta-analysis of rodent studies. Neurosci. Biobehav. Rev. 102, 299–307. https://doi.org/10.1016/j.neubiorev.2019.04.021.

Brake, W.G., Zhang, T.Y., Diorio, J., Meaney, M.J., Gratton, A., 2004. Influence of early postnatal rearing conditions on mesocorticolimbic dopamine and behavioural responses to psychostimulants and stressors in adult rats. Eur. J. Neurosci. 19, 1863–1874. https://doi.org/10.1111/j.1460-9568.2004.03286.x.

Chergui, K., Charléty, P.J., Akaoka, H., Saunier, C.F., Brunet, J.L., Buda, M., et al., 1993. Tonic activation of NMDA receptors causes spontaneous burst discharge of rat midbrain dopamine neurons in vivo. Eur. J. Neurosci. 5, 137–144. https://doi.org/10.1111/j.1460-9568.1993.tb00479.x.

Chocyk, A., Majcher-Maślanka, I., Przyborowska, A., Maćkowiak, M., Wedzony, K., 2015. Early-life stress increases the survival of midbrain dopamine neurons during postnatal development and enhances reward-related and anxiolytic-like behaviors in a sex-dependent fashion. Int. J. Dev. Neurosci. 44, 33–47. https://doi.org/10.1016/j.ijdevneu.2015.05.002.

Chocyk, A., Przyborowska, A., Dudys, D., Majcher, I., Maćkowiak, M., Wedzony, K., 2011. The impact of maternal separation on the number of tyrosine hydroxylase-expressing midbrain neurons during different stages of ontogenesis. Neuroscience 182, 43–61. https://doi.org/10.1016/j.neuroscience.2011.03.008.

Danielewicz, J., Hess, G., 2014. Early life stress alters synaptic modification range in the rat lateral amygdala. Behav. Brain Res. 265, 32–37. https://doi.org/10.1016/j.bbr.2014.02.012.

Douma, E.H., de Kloet, E.R., 2020. Stress-induced plasticity and functioning of ventral tegmental dopamine neurons. Neurosci. Biobehav. Rev. 108, 48–77. https://doi.org/10.1016/j.neubiorev.2019.10.015.

de Jong, J.W., Afjei, S.A., Pollak Dorocic, I., Peck, J.R., Liu, C., Kim, C.K., et al., 2019. A neural circuit mechanism for encoding aversive stimuli in the mesolimbic dopamine system. Neuron 101, 133–151. https://doi.org/10.1016/j.neuron.2018.11.005.

Fergusson, D.M., Woodward, L.J., Horwood, L.J., 2000. Risk factors and life processes associated with the onset of suicidal behaviour during adolescence and early adulthood. Psychol. Med. 30, 23–39. https://doi.org/10.1017/S003329179900135X.

Fitzgerald, L.W., Ortiz, J., Hamedani, A.G., Nestler, E.J., 1996. Drugs of abuse and stress increase the expression of GIuRI and NMDAR1 glutamate receptor subunits in the rat ventral tegmental area: common adaptations among cross-sensitizing agents. J. Neurosci. 16, 274–282. https://doi.org/10.1523/jneurosci.16-01-00274.1996.

Forster, G.L., Anderson, E.M., Scholl, J.L., Lukkes, J.L., Watt, M.J., 2018. Negative consequences of early-life adversity on substance use as mediated by corticotropin-releasing factor modulation of serotonin activity. Neurobiol. Stress 9, 29–39. https://doi.org/10.1016/j.ynstr.2018.08.001.

Gee, D.G., Casey, B.J., 2015. The impact of developmental timing for stress and recovery. Neurobiol. Stress 1, 184–194. https://doi.org/10.1016/j.ynstr.2015.02.001.

Geisler, S., Derst, C., Veh, R.W., Zahm, D.S., 2007. Glutamatergic afferents of the ventral tegmental area in the rat. J. Neurosci. 27, 5730–5743. https://doi.org/10.1523/JNEUROSCI.0012-07.2007.

Gershon, A., Sudheimer, K., Tirouvanziam, R., Williams, L.M., O'Hara, R., 2013. The long-term impact of early adversity on late-life psychiatric disorders. Curr. Psychiatr. Rep. 15 https://doi.org/10.1007/s11920-013-0352-9.

Gipson, C.D., Olive, M.F., 2017. Structural and functional plasticity of dendritic spines – root or result of behavior? Genes. Brain Behav 16, 101–117. https://doi.org/10.1111/gbb.12324.

Gondré-Lewis, M.C., Darius, P.J., Wang, H., Allard, J.S., 2016. Stereological analyses of reward system nuclei in maternally deprived/separated alcohol drinking rats. J. Chem. Neuroanat. 76, 122–132. https://doi.org/10.1016/j.jchemneu.2016.02.004.

Green, J.G., McLaughlin, K.A., Berglund, P.A., Gruber, M.J., Sampson, N.A., Zaslavsky, A.M., et al., 2010. Childhood adversities and adult psychiatric disorders in the national comorbidity survey replication I: associations with first onset of DSM-IV disorders. Arch. Gen. Psychiatry. 67, 113–123. https://doi.org/10.1001/archgenpsychiatry.2009.186.

Gunnar, M.R., Donzella, B., 2002. Social regulation of the cortisol levels in early human development. Psychoneuroendocrinology 27, 199–220. https://doi.org/10.1016/S0306-4530(01)00045-2.

Harfstrand, A., Fuxe, K., Cintra, A., Agnati, L.F., Zini, I., Wikström, A.C., et al., 1986. Glucocorticoid receptor immunoreactivity in monoaminergic neurons of rat brain. Proc. Natl. Acad. Sci. U.S.A. 83, 9779–9783. https://doi.org/10.1073/pnas.83.24.9779.

Heim, C., Newport, D.J., Mletzko, T., Miller, A.H., Nemeroff, C.B., 2008. The link between childhood trauma and depression: insights from HPA axis studies in humans. Psychoneuroendocrinology 33, 693–710. https://doi.org/10.1016/j.psyneuen.2008.03.008.

Heim, C., Newport, D.J., Wagner, D., Wilcox, M.M., Miller, A.H., Nemeroff, C.B., 2002. The role of early adverse experience and adulthood stress in the prediction of neuroendocrine stress reactivity in women: a multiple regression analysis. Depress. Anxiety 15, 117–125. https://doi.org/10.1002/da.10015.

Hikosaka, O., 2010. The habenula: from stress evasion to value-based decision-making. Nat. Rev. Neurosci. 11, 503–513. https://doi.org/10.1038/nrn2866.

Holly, E.N., Miczek, K.A., 2016. Ventral tegmental area dopamine revisited: effects of acute and repeated stress. Psychopharmacology (Berlin) 233, 163–186. https://doi.org/10.1007/s00213-015-4151-3.

Horii-Hayashi, N., Sasagawa, T., Matsunaga, W., Matsusue, Y., Azuma, C., Nishi, M., 2013. Developmental changes in desensitisation of c-fos expression induced by repeated maternal separation in pre-weaned mice. J. Neuroendocrinol. 25, 158–167. https://doi.org/10.1111/j.1365-2826.2012.02377.x.

Jahng, J.W., Ryu, V., Yoo, S.B., Noh, S.J., Kim, J.Y., Lee, J.H., 2010. Mesolimbic dopaminergic activity responding to acute stress is blunted in adolescent rats that experienced neonatal maternal separation. Neuroscience 171, 144–152. https://doi.org/10.1016/j.neuroscience.2010.08.063.

Jang, M., Bum Um, K., Jang, J., Jin Kim, H., Cho, H., Chung, S., et al., 2015. Coexistence of glutamatergic spine synapses and shaft synapses in substantia nigra dopamine neurons. Sci. Rep. 5 https://doi.org/10.1038/srep14773.

Jezierski, G., Zehle, S., Bock, J., Braun, K., Gruss, M., 2007. Early stress and chronic methylphenidate cross-sensitize dopaminergic responses in the adolescent medial prefrontal cortex and nucleus accumbens. J. Neurochem. 103, 2234–2244. https://doi.org/10.1111/j.1471-4159.2007.04927.x.

Juarez, B., Han, M.H., 2016. Diversity of dopaminergic neural circuits in response to drug exposure. Neuropsychopharmacology 41, 2424–2446. https://doi.org/10.1038/npp.2016.32.

Kasanova, Z., Hernaus, D., Vaessen, T., van Amelsvoort, T., Winz, O., Heinzel, A., et al., 2016. Early-life stress affects stress-related prefrontal dopamine activity in healthy adults, but not in individuals with psychotic disorder. PloS One 11, e0150746. https://doi.org/10.1371/journal.pone.0150746.

Kessler, R.C., Davis, C.G., Kendler, K.S., 1997. Childhood adversity and adult psychiatric disorder in the US National Comorbidity Survey. Psychol. Med. 27, 1101–1119. https://doi.org/10.1017/S0033291797005588.

Kuhlman, K.R., Geiss, E.G., Vargas, I., Lopez-Duran, N.L., 2015. Differential associations between childhood trauma subtypes and adolescent HPA-axis functioning. Psychoneuroendocrinology 54, 103–114. https://doi.org/10.1016/j.psyneuen.2015.01.020.

Kuhlman, K.R., Vargas, I., Geiss, E.G., Lopez-Duran, N.L., 2015a. Age of trauma onset and HPA Axis dysregulation among trauma-exposed youth. J. Trauma Stress 28, 572–579. https://doi.org/10.1002/jts.22054.

Lammel, S., Ion, D.I., Roeper, J., Malenka, R.C., 2011. Projection-specific modulation of dopamine neuron synapses by aversive and rewarding stimuli. Neuron 70, 855–862. https://doi.org/10.1016/j.neuron.2011.03.025.

Lammel, S., Lim, B.K., Malenka, R.C., 2014. Reward and aversion in a heterogeneous midbrain dopamine system. Neuropharmacology 76, 351–359. https://doi.org/10.1016/j.neuropharm.2013.03.019.

Lammel, S., Lim, B.K., Ran, C., Huang, K.W., Betley, M.J., Tye, K., et al., 2012. Input-specific control of reward and aversion in the ventral tegmental area HHS Public Access. Nature 491, 212–217. https://doi.org/10.1038/nature11527.

Lippmann, M., Bress, A., Nemeroff, C.B., Plotsky, P.M., Monteggia, L.M., 2007. Long-term behavioural and molecular alterations associated with maternal separation in rats. Eur. J. Neurosci. 25, 3091–3098. https://doi.org/10.1111/j.1460-9568.2007.05522.x.

Lisman, J.E., Grace, A.A., 2005. The hippocampal-VTA loop: controlling the entry of information into long-term memory. Neuron 46, 703–713. https://doi.org/10.1016/j.neuron.2005.05.002.

Longair, M.H., Baker, D.A., Armstrong, J.D., 2011. Simple neurite tracer: open source software for reconstruction, visualization and analysis of neuronal processes. Bioinformatics 27, 2453–2454. https://doi.org/10.1093/bioinformatics/btr390.

Majcher-Maślanka, I., Solarz, A., Wędzony, K., Chocyk, A., 2017. The effects of early-life stress on dopamine system function in adolescent female rats. Int. J. Dev. Neurosci. 57, 24–33. https://doi.org/10.1016/j.ijdevneu.2017.01.001.

Margolis, E.B., Lock, H., Hjelmstad, G.O., Fields, H.L., 2006. The ventral tegmental area revisited: is there an electrophysiological marker for dopaminergic neurons? J. Physiol. 577, 907–924. https://doi.org/10.1113/jphysiol.2006.117069.

Marusak, H.A., Hatfield, J.R.B., Thomason, M.E., Rabinak, C.A., 2017. Reduced ventral tegmental area–hippocampal connectivity in children and adolescents exposed to early threat. Biol. Psychiatry Cogn. Neurosci. Neuroimaging 2, 130–137. https://doi.org/10.1016/j.bpsc.2016.11.002.

Masrouri, H., Azadi, M., Semnanian, S., Azizi, H., 2020. Maternal deprivation induces persistent adaptations in putative dopamine neurons in rat ventral tegmental area: in vivo electrophysiological study. Exp. Brain Res. 1, 3. https://doi.org/10.1007/s00221-020-05884-x.

Matthews, K., Dalley, J.W., Matthews, C., Tsai, T.H., Robbins, T.W., 2001. Periodic maternal separation of neonatal rats produces region- and gender-specific effects on biogenic amine content in postmortem adult brain. Synapse 40, 1–10. https://doi.org/10.1002/1098-2396(200104)40:1<1::AID-SYN1020>3.0.CO;2-E.

Meaney, M.J., Brake, W., Gratton, A., 2002. Environmental regulation of the development of mesolimbic dopamine systems: a neurobiological mechanism for vulnerability to drug abuse? Psychoneuroendocrinology 27, 127–138. https://doi.org/10.1016/s0306-4530(01)00040-3.

Morales, M., Margolis, E.B., 2017. Ventral tegmental area: cellular heterogeneity, connectivity and behaviour. Nat. Rev. Neurosci. 18, 73–85. https://doi.org/10.1038/nrn.2016.165.

Nakahata, Y., Yasuda, R., 2018. Plasticity of spine structure: Local signaling, translation and cytoskeletal reorganization. Front. Synaptic Neurosci. 10 https://doi.org/10.3389/fnsyn.2018.00029.

Nishi, M., Horii-Hayashi, N., Sasagawa, T., 2014. Effects of early life adverse experiences on the brain: implications from maternal separation models in rodents. Front. Neurosci. 8, 166. https://doi.org/10.3389/fnins.2014.00166.

Novick, A.M., Levandowski, M.L., Laumann, L.E., Philip, N.S., Price, L.H., Tyrka, A.R., 2018. The effects of early life stress on reward processing. J. Psychiatr. Res. 101, 80–103. https://doi.org/10.1016/j.jpsychires.2018.02.002.

Overton, P.G., Tong, Z.Y., Brain, P.F., Clark, D., 1996. Preferential occupation of mineralocorticoid receptors by corticosterone enhances glutamate-induced burst firing in rat midbrain dopaminergic neurons. Brain Res. 737, 146–154. https://doi.org/10.1016/0006-8993(96)00722-6.

Peña, C.J., Kronman, H.G., Walker, D.M., Cates, H.M., Bagot, R.C., Purushothaman, I., et al., 2017. Early life stress confers lifelong stress susceptibility in mice via ventral tegmental area OTX2. Science 356, 1185–1188. https://doi.org/10.1126/science.aan4491.

Phillipson, O.T., 1979. A Golgi study of the ventral tegmental area of Tsai and interfascicular nucleus in the rat. J. Comp. Neurol. 187, 99–115. https://doi.org/10.1002/cne.901870107.

Piazza, P.V., Le Moal, M., 1998. The role of stress in drug self-administration. Trends Pharmacol. Sci. 19, 67–74. https://doi.org/10.1016/S0165-6147(97)01115-2.

Pignatelli, M., Bonci, A., 2015. Role of dopamine neurons in reward and aversion: a synaptic plasticity perspective. Neuron 86, 1145–1157. https://doi.org/10.1016/j.neuron.2015.04.015.

Polter, A.M., Kauer, J.A., 2014. Stress and VTA synapses: implications for addiction and depression. Eur. J. Neurosci. 39, 1179–1188. https://doi.org/10.1111/ejn.12490.

Pruessner, J.C., Champagne, F., Meaney, M.J., Dagher, A., 2004. Dopamine release in response to a psychological stress in humans and its relationship to early life maternal care: a positron emission tomography study using [11C]raclopride. J. Neurosci. 24, 2825–2831. https://doi.org/10.1523/JNEUROSCI.3422-03.2004.

Rees, S.L., Steiner, M., Fleming, A.S., 2006. Early deprivation, but not maternal separation, attenuates rise in corticosterone levels after exposure to a novel environment in both juvenile and adult female rats. Behav. Brain Res. 175, 383–391. https://doi.org/10.1016/j.bbr.2006.09.013.

Rodriguez, A., Ehlenberger, D.B., Dickstein, D.L., Hof, P.R., Wearne, S.L., 2008. Automated three-dimensional detection and shape classification of dendritic spines from fluorescence microscopy images. PloS One 3. https://doi.org/10.1371/journal.pone.0001997.

Salamone, J.D., Yohn, S.E., López-Cruz, L., San Miguel, N., Correa, M., 2016. Activational and effort-related aspects of motivation: neural mechanisms and implications for psychopathology. Brain 139, 1325–1347. https://doi.org/10.1093/brain/aww050.

Sarti, F., Borgland, S.L., Kharazia, V.N., Bonci, A., 2007. Acute cocaine exposure alters spine density and long-term potentiation in the ventral tegmental area. Eur. J. Neurosci. 26, 749–756. https://doi.org/10.1111/j.1460-9568.2007.05689.x.

Schneider, C.A., Rasband, W.S., Eliceiri, K.W., 2012. NIH Image to ImageJ: 25 years of image analysis. Nat. Methods 9, 671–675. https://doi.org/10.1038/nmeth.2089.

Scorcioni, R., Polavaram, S., Ascoli, G.A., 2008. L-Measure: a web-accessible tool for the analysis, comparison and search of digital reconstructions of neuronal morphologies. Nat. Protoc. 3, 866–876. https://doi.org/10.1038/nprot.2008.51.

Shepard, R.D., Langlois, L.D., Authement, M.E., Nugent, F.S., 2020. Histone deacetylase inhibition reduces ventral tegmental area dopamine neuronal hyperexcitability involving AKAP150 signaling following maternal deprivation in juvenile male rats. J. Neurosci. Res. 98, 1457–1467. https://doi.org/10.1002/jnr.24613.

Sola, E., Prestori, F., Rossi, P., Taglietti, V., D'Angelo, E., 2004. Increased neurotransmitter release during long-term potentiation at mossy fibre-granule cell synapses in rat cerebellum. J. Physiol. 557, 843–861. https://doi.org/10.1113/jphysiol.2003.060285.

Spear, L.P., 2000. The adolescent brain and age-related behavioral manifestations. Neurosci. Biobehav. Rev. 24, 417–463. https://doi.org/10.1016/S0149-7634(00)00014-2.

Stamatakis, A.M., Jennings, J.H., Ung, R.L., Blair, G.A., Weinberg, R.J., Neve, R.L., et al., 2013. A unique population of ventral tegmental area neurons inhibits the lateral habenula to promote reward. Neuron 80, 1039–1053. https://doi.org/10.1016/j.neuron.2013.08.023.

Stuart, S.A., Hinchcliffe, J.K., Robinson, E.S.J., 2019. Evidence that neuropsychological deficits following early life adversity may underlie vulnerability to depression. Neuropsychopharmacology 44, 1623–1630. https://doi.org/10.1038/s41386-019-0388-6.

Ungless, M.A., Grace, A.A., 2012. Are you or aren't you? Challenges associated with physiologically identifying dopamine neurons. Trends Neurosci. 35, 422–430. https://doi.org/10.1016/j.tins.2012.02.003.

Ungless, M.A., Magill, P.J., Bolam, J.P., 2004. Uniform inhibition of dopamine neurons in the ventral tegmental area by aversive stimuli. Science 303, 2040–2042. https://doi.org/10.1126/science.1093360.

World Health Organization, 2020. https://www.who.int/en/news-room/fact-sheets/detail/child-maltreatment. (Accessed 20 June 2020).

Zweifel, L.S., Parker, J.G., Lobb, C.J., Rainwater, A., Wall, V., Fadok, J.P., et al., 2009. Disruption of NMDAR-dependent burst firing by dopamine neurons provides selective assessment of phasic dopamine-dependent behavior. Proc. Natl. Acad. Sci. U.S.A. 106, 7281–7288. https://doi.org/10.1073/pnas.0813415106.